Vibrationally Resolved *K*-shell Photoionization of CO with Circularly Polarized Light

T. Jahnke,[1,*] L. Foucar,[1] J. Titze,[1] R. Wallauer,[1] T. Osipov,[2] E. P. Benis,[2] A. Alnaser,[2] O. Jagutzki,[1] W. Arnold,[1]
S. K. Semenov,[3] N. A. Cherepkov,[3] L. Ph. H. Schmidt,[1] A. Czasch,[1] A. Staudte,[1] M. Schöffler,[1] C. L. Cocke,[2] M. H. Prior,[4]
H. Schmidt-Böcking,[1] and R. Dörner[1]

[1]*Institut für Kernphysik, University of Frankfurt, August-Euler Str. 6, D-60486 Frankfurt, Germany*
[2]*Dept. of Physics, Kansas State University, Cardwell Hall, Manhattan, Kansas, 66506, USA*
[3]*State University of Aerospace Instrumentation, 190000 St. Petersburg, Russia*
[4]*Lawrence Berkeley National Laboratory, Berkeley, California, 94720, USA*
(Received 22 January 2004; published 19 August 2004)

Diffraction of a low energy (< 4 eV) carbon-*K*-photoelectron wave that is created inside a CO molecule by absorption of a circularly polarized photon is investigated. The measurements resolve the vibrational states of the *K*-shell ionized CO^+ molecule and display the photoelectron diffraction patterns in the molecular frame. These show significant variation for the different vibrational states. This effect is stronger than predicted by state-of-the-art theory. As this study is performed close to C-*K*-threshold and, therefore, far below the molecule's σ-shape resonance, this surprisingly strong effect is not related to that resonance phenomenon.

Methods of measuring molecular frame photoelectron angular distributions from small molecules in the gas phase have been established successfully during the last eight years in several experiments [1–5]. These have revealed rich angular structures that can be understood as the diffraction patterns of the scattered photoelectron waves propagating in the molecular potential. The diffraction pattern varies with the wavelength of the photoelectron and has been predicted to depend strongly on the details of the molecular potential and the internuclear distance [6]. Analysis of x-ray photoelectron diffraction from surfaces makes use of this prediction to determine bond lengths; thus a direct observation in isolated molecules is especially valuable as a fundamental test of this application of theory.

In the present Letter we experimentally explore the dependence of the low energy photoelectron diffraction of carbon- *K*-shell photoelectrons from CO on the internuclear distance. This is achieved by resolving the vibrational levels of the CO^+ ion in the energy of the photoelectrons while measuring their vector momenta in the molecular frame.

Figure 1 shows the potential curves of the ground state of CO and the core ionized $C(1s^{-1})O^+$ together with the nuclear wave function and the products of the initial and final state nuclear wave functions. In photoionization events the first three vibrational levels of $C(1s^{-1})O^+$ are populated in a vertical transition from the CO ground state; i.e., the photoelectron energy indicates the $C(1s^{-1})O^+$ vibrational state. The equilibrium distance of the ionized state is about 4.5% smaller than that of the ground state (1.079 Å a.u. compared to 1.128 Å a.u. [7]). Therefore, as shown in Fig. 1, a vertical transition populates several vibrational states. Selecting photoelectrons of a given vibrational line thus samples a particular fraction of internuclear distances.

Dehmer et al. [6] have shown theoretically that the position of the shape resonance and the beta parameter of the photoelectron depend on the vibrational state. This prediction has been verified experimentally by Köppe et al. [8]. Very recently Adachi et al. [9] have shown that on the shape resonance the photoelectron angular distribution changes with the vibrational level. Our study is performed at energies within a few eV above threshold and hence well below the σ-shape resonance which is about 10 eV higher. We thereby demonstrate that this phenomenon is a more general one and not related to
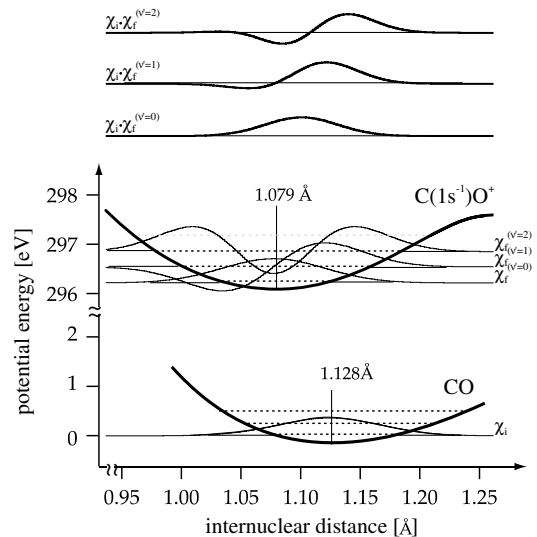

FIG. 1. Ground vibrational state of CO and the first vibrational states of carbon-*K*-ionized CO^+. The equilibrium internuclear distances are 1.128 Å and 1.079 Å [7], and the vibrational spacings are 269 and 301 meV [14] for CO and CO^+, respectively. Top: products of the CO ground state and CO^+ vibrational wave functions.

the shape resonance. Comparison with state-of-the-art theory shows that it is much stronger than predicted.

The experiment was performed in the following way: a supersonic CO jet intersected a beam of circularly polarized light ($S = 0.99$) at beam line 4.0.2 of the Advanced Light Source at Lawrence Berkeley National Laboratory. The COLTRIMS (cold target recoil ion momentum spectroscope) technique [10] was used to measure the momenta and charge states of the CO fragments in coincidence with the vector momentum of the ejected photoelectron. Homogenous electric and magnetic fields were applied to guide the photo fragments from the interaction region onto two position sensitive delay line detectors [11]. By measuring the time-of-flight and the position of impact of each particle, we derive their initial vector momenta by reconstructing their trajectories. An acceptance solid angle of 4π is achieved for photoelectrons up to 4 eV and for photoions with a kinetic energy of up to 8 eV. In most cases the $C(1s^{-1})O^{+}$ ion undergoes an Auger decay and the resulting CO^{2+} ion breaks into two singly charged fragments. Other decay channels are possible as well, leading to multiply charged fragments or an intact CO^{2+} ion. We measured two ionic fragments and the photoelectron in triple coincidence. Furthermore, in the analysis, only those events which led to C^{+} and O^{+} fragments with a total kinetic energy release (KER) 10.5 eV were included, as the axial recoil approximation has been shown to be valid for KERs of this magnitude [12]. Hence, for each photoionization event, the orientation of the molecule at the instant of photo-absorption is determined by the measured relative momentum vector of the ionic fragments.

In order to capture fragments with high KER, an electric field of 10.2 V/cm was used. The magnetic field of 2.78 G was chosen for the experiments at 297.3 and 298.3 eV photon energy. For energies of 299.3 eV and 300.7 eV the B-field was altered to 4.01 G. The fields were chosen in order to optimize the electron energy resolution of the COLTRIMS-spectrometer. Since the energy resolution of this type of spectrometer is different for momenta parallel and perpendicular to the electric field, we used only events with electrons emitted within $90^{o} \pm 30^{o}$ with respect to the spectrometer axis. In that case, and for the chosen settings of magnetic and electric fields, the photoelectron energy resolution was 66 meV at 2 eV and 150 meV at 4 eV photoelectron energy, respectively.

Figure 2 shows the photoelectron energy distribution for a photon energy of 298.3 eV consisting of the photo lines of the three lowest vibrational states of the CO^{+} molecule with a carbon-K-shell hole. The line shape in this energy region is strongly influenced by post collision interaction (PCI) effects that occur due to the interaction of the photoelectron and the emitted Auger electron. Therefore the expected Lorentzian shape of the photo

line is smeared out towards lower energies while the energy of the Auger electron is increased. The resulting distortion of the line shape can be described semiclassically as shown by Morgenstern et al. who derived the shape of PCI-effected Auger lines in [13]. The solid line is a fit of a sum of three PCI-distorted Lorentz-distributions. In order to include the experimental resolution, a Gaussian with a FWHM of 120 meV is convoluted with the PCI line shape from [13]; this accounts for the photon energy resolution of 100 meV and a mean resolution of 66 meV of the COLTRIMS analyzer. Our measured fraction of the vibrational levels to the total cross section is 50% for $\nu' = 0$, 35% for $\nu' = 1$, and 15% for $\nu' = 2$ which is consistent to the values reported in [14]. Contributions from higher ν' are known to be small in this energy region and have therefore been neglected in our fitting procedure [8].

To obtain the molecular frame angular distributions of the photoelectrons, the partial contribution of each vibrational state to the photoelectron energy spectrum has been obtained by performing the fit shown in Fig. 2 for every angle in the molecular frame that is plotted. PCI effects on the line shape can depend of the relative angle of photo and Auger electrons, provided their energies are of the same order of magnitude. In our case, the Auger electron energy is much larger than the photoelectron energy; and in addition, the direction of Auger electron emission is not fixed. Therefore we assume the line shape to be angularly independent . The resulting vibrationally resolved molecular frame angular distributions are shown in Fig. 3 for 4 photon energies.
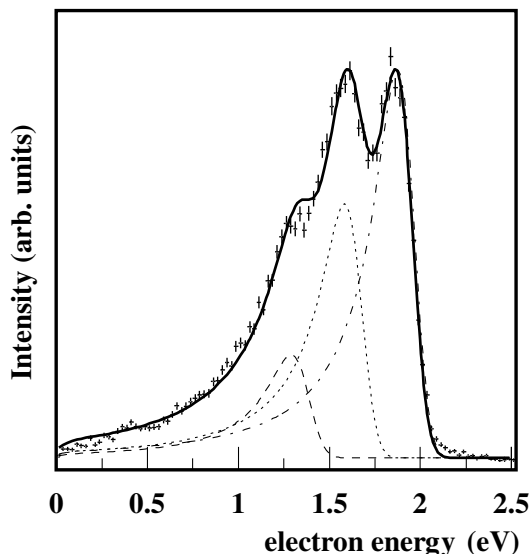

FIG. 2. C-K-photoelectron (carbon-K-shell) energy distribution as created by photons of 298.3 eV energy. The solid line is a sum of the photo lines of the contributing vibrational CO^{+} states (dotted lines), represented by distorted Lorentz shapes according to [13].

We find a strong circular dichroism as already seen for the vibrationally unresolved case in [15]. However, a surprisingly strong dependence of the angular distribution on the vibrational level is observed. As already mentioned, the photoelectrons studied in this work are, in all cases, energetically well below the maximum of the σ-shape resonance, making it unlikely that the observed variations originate from that resonance phenomenon.

Depending on the photon energy below the σ-shape resonance, doubly excited CO states can be populated that produce, via autoionization, a CO^+ ion, as does the direct photoionization channel. Thus electrons originating from these photo-excitation events cannot be distinguished from photoelectrons from the direct process in the present experiment. It has been shown, however, that these doubly

excited states do not contribute in the photon energy region from C-K-threshold to $\sim$300.3 eV [8]. The photoelectron angular distributions shown in 3(a)–3(c) are therefore not affected by doubly excited states, while the distributions shown in 3(d) were acquired at a photon energy at which doubly excited states can be populated and hence may include electrons from their autoionization.

A feasible explanation for the observed dependence of the photoelectron angular distribution on the ion's vibrational level may be found in the variation of the molecular potential for different internuclear distances: as first shown by Dehmer and Dill [6], the electron angular distribution ($I(\vartheta_e, \phi_e)$) for a given vibrational final state ν^l and a certain molecular direction ϑ_m can be expressed
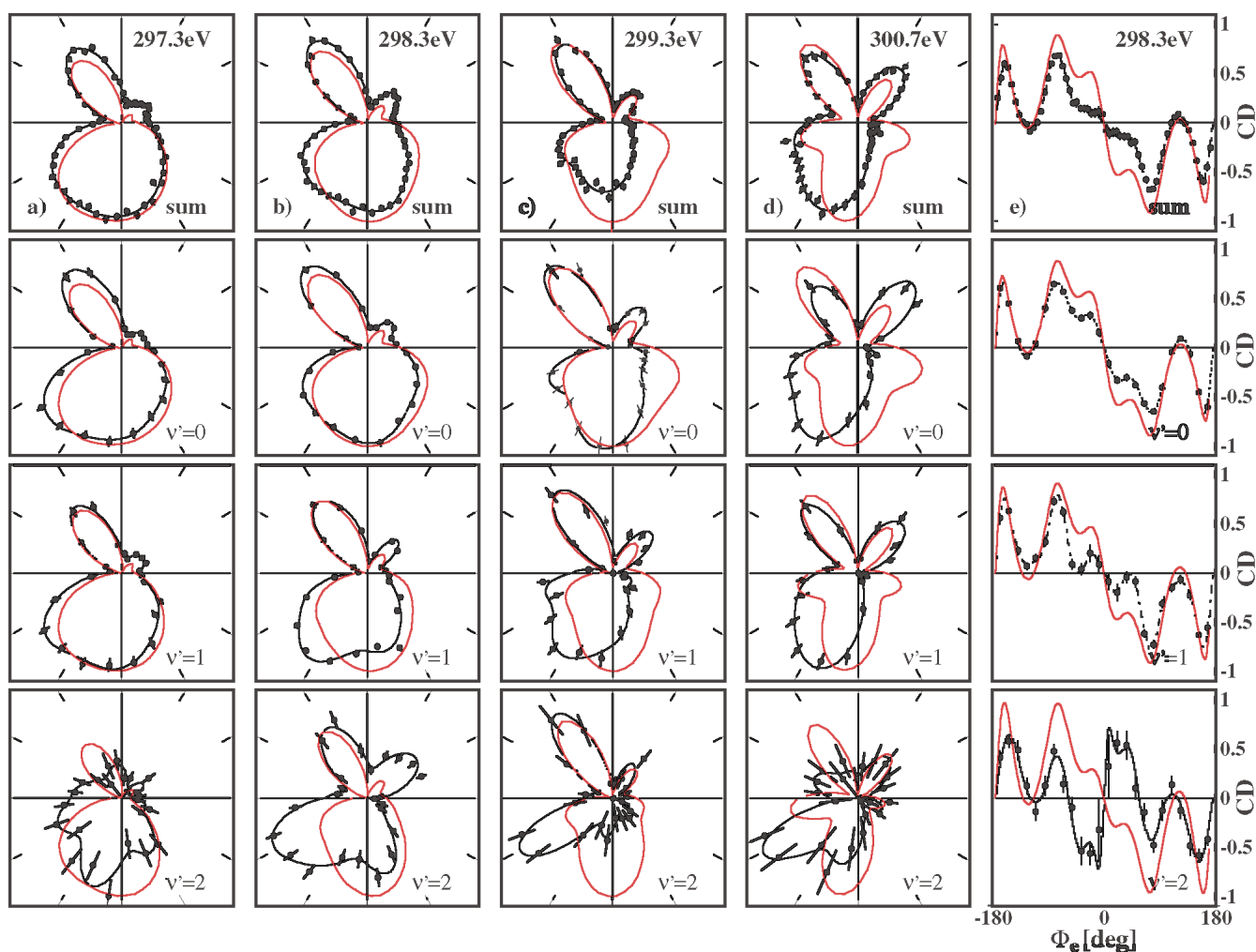

FIG. 3 (color online). Molecular frame photoelectron distributions for (a) 297.3 eV, (b) 298.3 eV, (c) 299.3 eV, and (d) 300.7 eV photon energy. Column (e) shows the circular dichroism (CD, the normalized difference between the angular distribution obtained for left and right circularly polarized light) at a photon energy of 298.3 eV. Top to bottom: angular distribution for the sum of all vibrational states, those for $\nu^l = 0$, $\nu^l = 1$, $\nu^l = 2$. The molecule is oriented horizontally within the plane of the figure with the O atom to the left. Furthermore, the paper plane corresponds to the polarization plane of the left hand circularly polarized photons propagating into the plane. Grey line: relaxed core HF calculations normalized to the maximum of the experimental distribution. The black line shows a fit of spherical harmonics up to $l = 5$.

within the Franck-Condon principle as:

$$I^{\nu'}(\omega, \vartheta_e, \phi_e, \vartheta_m) = | \int \chi_f^{\nu'}(R) d(R, \omega, \vartheta_e, \phi_e, \vartheta_m)$$

$$\times \chi_i^{\nu}(R) dR|^2. \qquad (1)$$

The electronic transition matrix element $d(R, \omega, \vartheta_e, \phi_e, \vartheta_m)$ at a given internuclear distance R is weighted with the product of the initial and final state nuclear wave function. This product is shown in Fig. 1. The mean internuclear distance between $\chi_i \cdot \chi_f$ for the $\nu' = 0$ and $\nu' = 1$ vibrational state differs by only 2.1 %; however, this small change yields observable differences in the photoelectron angular distributions. For the $\nu' = 2$, the situation is different. Since the transition matrix element varies continuously with changing internuclear distance, the contributions from close to the zero crossing of $\chi_i \cdot \chi_f^{(\nu'=2)}$ at 1.11 Å will vanish due to the change in sign of $\chi_i \cdot \chi_f^{(\nu'=2)}$. Therefore the $\nu' = 2$ state will have the strongest contribution from around 1.145 Å and a somewhat smaller contribution with opposite sign from internuclear distances of about 1.085 Å. The experimental data in Fig. 3 suggest that this fact leads to an even stronger change in the angular distributions between $\nu' = 1$ and $\nu' = 2$ than between $\nu' = 0$ and $\nu' = 1$.

The theoretical calculations in this Letter (Fig. 3, gray line) are restricted to the Hartree-Fock (HF) approximation since many electron correlations are small (as confirmed by calculations in RPA (random phase approximation) at equilibrium distance) and the C-K-shell is well separated in energy from the other shells so that intershell many electron correlations are also negligible. On the other hand, the effect of core relaxation after ejection of one electron must be taken into account [16]. This is done in the framework of the Relaxed Core HF (RCHF) approximation [17].

The calculations described above have been performed for several fixed internuclear distances R, giving a set of the dipole matrix elements $d(\omega, R)$ for each photon energy ω. To obtain $I^{\nu'}(\omega, \vartheta_e, \phi_e, \vartheta_m)$ for a vibrationally resolved transition, the matrix elements were multiplied by the corresponding initial and final vibrational state wave functions, χ_ν and $\chi_{\nu'}$, and integrated over the internuclear distance R as shown in Eq. (1).

Note that under the experimental conditions only the initial state ground vibrational level $\nu = 0$ is populated. We integrated over R using 11 points around the equilibrium distance $R = 1.128$ Å of the ground state [18] with steps of 0.0265 Å (0.05 a.u.).

The failure of our theory to reproduce the observed sharp variation of the angular distributions with increasing vibrational quantum number ν' is most probably related to the approximate way in which the core relaxation effect is taken into account. Because of that, the relative contributions of different partial waves are not reproduced correctly. In particular, it is likely that the relative contribution of the d_σ partial wave is increasing with ν' faster than it is given by our theory.

Our present study suggests that the agreement between measured vibrationally averaged, molecular frame, photoelectron angular distributions and theoretical calculations, mostly in the fixed nuclei approximation, is somewhat fortuitous. For the more differential, vibrationally resolved cases the agreement is far from satisfactory. The studies in this Letter were carried out in a photon energy region close to the C-K-threshold where neither doubly excited CO^+ states nor influences of the molecule's σ-shape resonance make significant contributions, suggesting that the observed effects are due to the changes in the contributing internuclear separations and the resultant variations of the molecular potential for the different vibrational levels of the carbon-K-shell ionized CO^+ ground state.

———————

*Electronic address: jahnke@hsb.uni-frankfurt.de
[1] A. V. Golovin, N. A. Cherepkov, and V. V. Kuznetsov, Z. Phys. D: At., Mol. Clusters **24**, 371 (1992).
[2] E. Shigemasa *et al.*, Phys. Rev. Lett., **74**, 359 (1995).
[3] F. Heiser *et al.*, Phys. Rev. Lett. **79**, 2435 (1997).
[4] A. Lafosse *et al.*, Phys. Rev. Lett. **84**, 5987 (2000).
[5] A. L. Landers *et al.*, Phys. Rev. Lett. **87**, 013002 (2001).
[6] J. L. Dehmer, D. Dill, and S. Wallace, Phys. Rev. Lett. **43**, 1005 (1979).
[7] B. Kempgens *et al.*, J. Phys. B **30**, L741 (1997).
[8] H. M. Köppe *et al.*, Chem. Phys. Lett. **260**, 223 (1996).
[9] J. Adachi *et al.*, Phys. Rev. Lett. **91**, 163001 (2003).
[10] R. Dörner *et al.*, Phys. Rep. **330**, 96 (2000).
[11] See http://www.Roentdek.com for details of the detectors.
[12] T. Weber *et al.*, J. Phys. B **34**, 3669 (2001).
[13] R. Morgenstern, A. Niehaus, and U. Thielmann, J. Phys. B **9**, L363 (1976).
[14] K. J. Randall *et al.*, Phys. Rev. Lett. **71**, 1156 (1993).
[15] T. Jahnke *et al.*, Phys. Rev. Lett. **88**, 073002 (2002).
[16] L. D. Lynch and V. McKoy, Phys. Rev. A **30**, 1561 (1984).
[17] S. K. Semenov and N. A. Cherepkov. Phys. Rev. A **66**, 022708 (2002).
[18] H. M. Köppe *et al.*, J. Electron Spectrosc. Relat. Phenom. **75**, 97 (1995).